Supporting Information

Nano-hetero-architectures of two-dimensional (2D) MoS_2@ one-dimensional (1D) brookite TiO_2 nanorods: prominent electron emitters for displays

Rupesh S. Devan,[a] Vishal P. Thakare,[b] Vivek V. Antad,[b,c] Parameshwar R. Chikate,[a] Ruchita T. Khare,[d] Mahendra A. More,[d] Rajendra S. Dhayal,[e] Shankar I. Patil,[d] Yuan-Ron Ma[f] and Lukas Schmidt-Mende[g]*

[a.] Discipline of Metallurgy Engineering & Materials Science, Indian Institute of Technology Indore, Simrol 453552, India; E-mail: devan_rs@yahoo.co.in & rupesh@iiti.ac.in

[b.] Physical & Materials Chemistry Division, CSIR-National Chemical Laboratory, Dr. Homi Bhabha Road, Pune 411008, India

[c.] Nowrosjee Wadia College of Arts and Science, 19, Late Prin. V. K. Joag Path, Pune - 411001, India.

[d.] Department of Physics, Savitribai Phule Pune University, (Formerly, University of Pune), Pune 411007, India

[e.] Centre for Chemical Sciences, School of Basics and Applied Sciences, Central University of Punjab, Bathinda, 151001, India

[f.] Department of Physics, National Dong Hwa University, Hualien 97401, Taiwan, R.O.C.

[g.] Department of Physics, University of Konstanz, Constance 78457, Germany

(A) Pure 2D MoS_2 layers and 2D MoS_2@1D β-TiO_2 nanorods

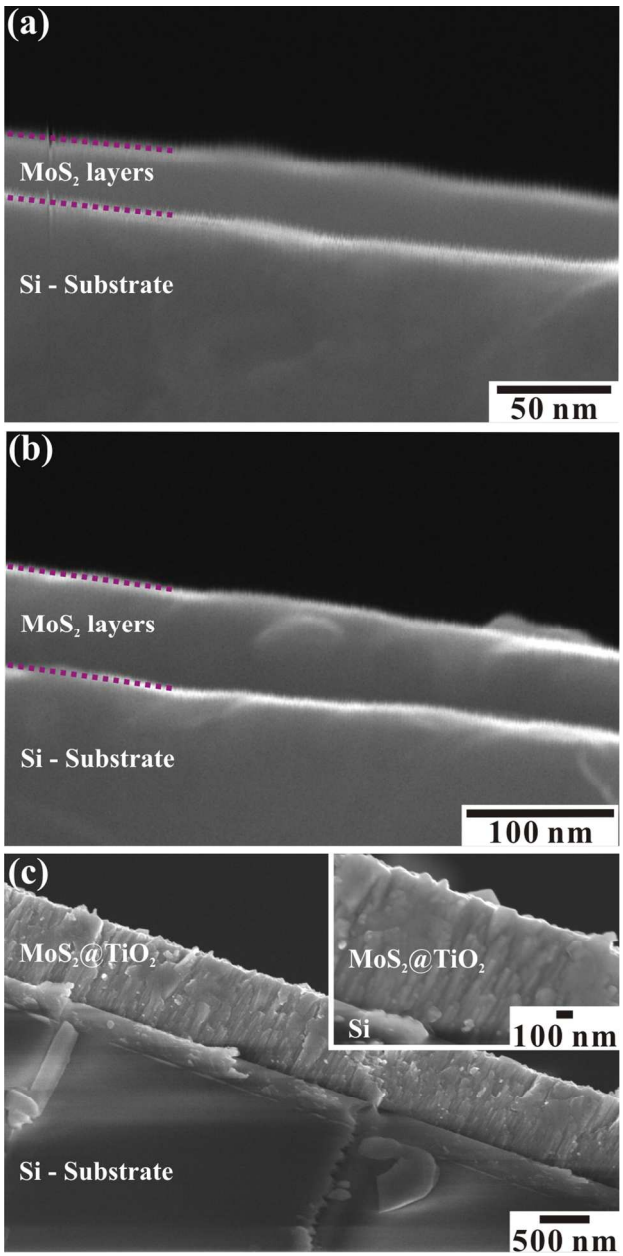

Figure S1. FESEM images showing the cross-sectional view of the large-area array of (a) ~ 20 (± 3) and (b) 40 (± 3) nm thick MoS_2 layers deposited over Si substrate at deposition rate of 500 and 1000 shots, respectively, and (c) 40 (± 3) nm thick MoS_2 layer loaded over 1D β-TiO_2 nanorods. The inset shows the high magnification FESEM image of the portion of 2D MoS_2@1D β-TiO_2 nanorods.

2D MoS_2 layers were deposited over pure Si substrate utilizing PLD technique at optimized conditions. The thickness of MoS_2 was calibrated and confirmed at these optimized conditions before subjected over 1D β-TiO_2 nanorods. High magnification FESEM images in Figure S1 (a and b) shows the cross-sectional views of the MoS_2 thin film produced over Si substrate at deposited rate of ~ 500 and 1000 shots, respectively. The thickness of ~40 (± 3) nm calibrated at 1000 shots (Figure S1 (b)) was further reduced to the ~20 (± 3) nm when the deposition was carried out at 500 shots. However, at a deposition rate of 100 shots, the thickness of MoS_2 layer over Si substrate was not clearly distinguishable in FESEM. Therefore, from the calibration of 1000 and 500 shots, it has unanimously been considered that the ~4 (± 2 nm) nm thick layers of MoS_2 might have produced over Si substrate at the deposition of 100 shots. After these calibrations, 2D MoS_2 layers of ~40 (± 3), 20 (± 3) and 4 (± 2) nm were subjected over 1D β-TiO_2 nanorods at their optimized conditions. Figure S1 (c) shows a cross-sectional view of the ~40 (± 3) nm thick MoS_2 loaded 1D β-TiO_2 nanorods. The 2D MoS_2 layers are formed along the textural boundaries of 1D β-TiO_2 nanorods to fill up the gaps present in between the 1D nanorods (observed in Figure 1(a)). The dense film of 2D MoS_2@1D β-TiO_2 nanorods was observed.

(B) Raman analysis of MoS_2@TiO_2

Raman spectroscopic analysis was employed to study the structural properties of the large area array of 2D MoS_2@1D β-TiO_2 nanorods. Figure S2 shows the Raman spectra for the array of 1D β-TiO_2 nanorods loaded with 40 nm thick layer of 2D MoS_2. There were three Raman bands observed at 218.6, 380.0 and 406.28 cm^{-1}. The existence of the brookite TiO_2 phase is confirmed from the peak observed at 218.6 cm^{-1}, which is assigned to the B_{1g} mode of brookite phase with the space group of D^{15}_{2h} (Pbca) in previous Raman studies of pristine TiO_2 thin films

and nanoparticles.[1-3] Furthermore, no peak observed at 513 cm^{-1} assigned to the anatase phase confirm the formation 1D TiO_2 nanorods of pure brookite phase.[4] The appearance of two prominent peaks at 380 and 406.28 cm^{-1} corresponds to the in-plane E_{2g} and out-of-plane A_{1g} vibration modes, respectively, of the 2D MoS_2.[5-7] The peak frequency difference (Δk) of 26.28 cm^{-1} observed between E_{2g} and A_{1g} confirm the single crystalline multilayer MoS_2 formation over 1D TiO_2 nanorods. These observations are akin to the results for single crystalline monolayer and multilayer of MoS_2 over a sapphire substrate[6] and MoS_2 multilayers exfoliated with various organolithium compounds.[7] This confirms that the 40 nm thick layer of 2D has been loaded over 1D TiO_2 nanorods to form nano-hetero-architecture of 2D MoS_2@1D β-TiO_2 nanorods.

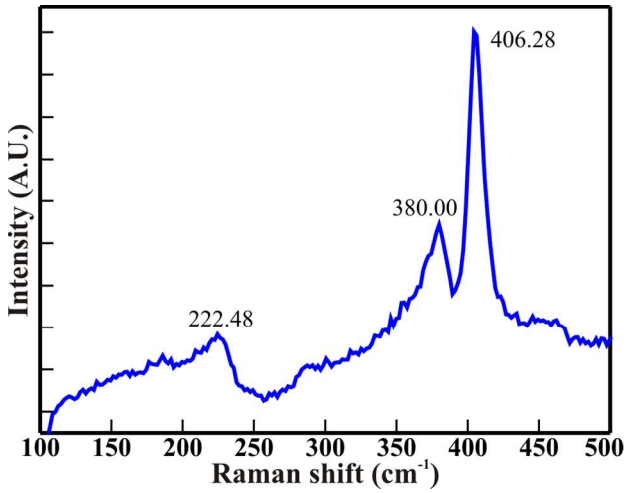

Figure S2. Raman spectrum of the large area array of 2D MoS_2@1D β-TiO_2 nanorods with 40 nm layer of MoS_2.

(C) XPS Analysis:

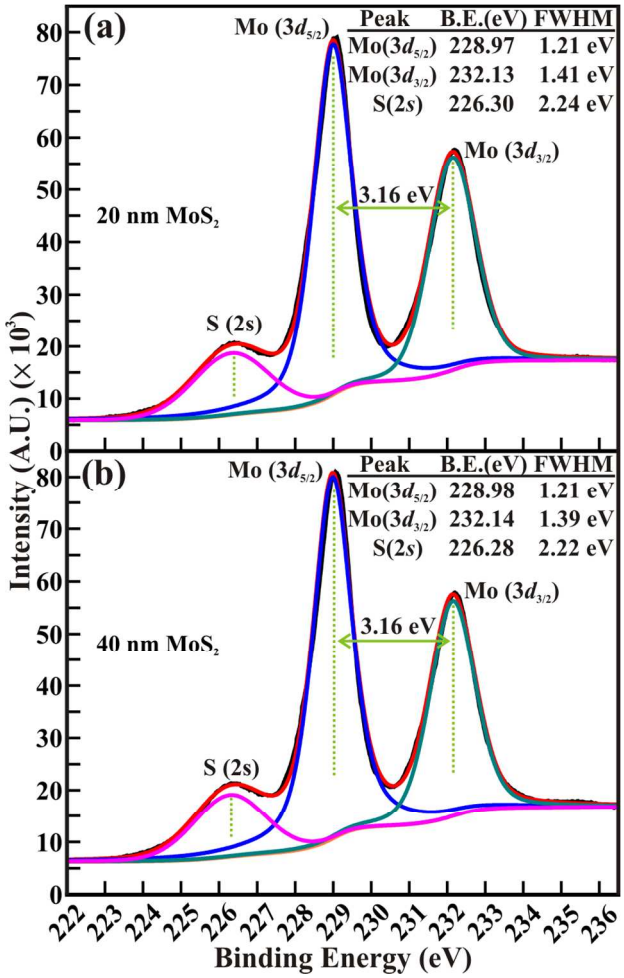

Figure S3. The deconvoluted XPS spectra of Mo (*3d*) core levels of (a) ~ 20 nm and (b) ~ 40 nm thick MoS_2 loaded β-TiO_2 nanorods. The XPS spectra are deconvoluted *via* Voigt curve function fitting.

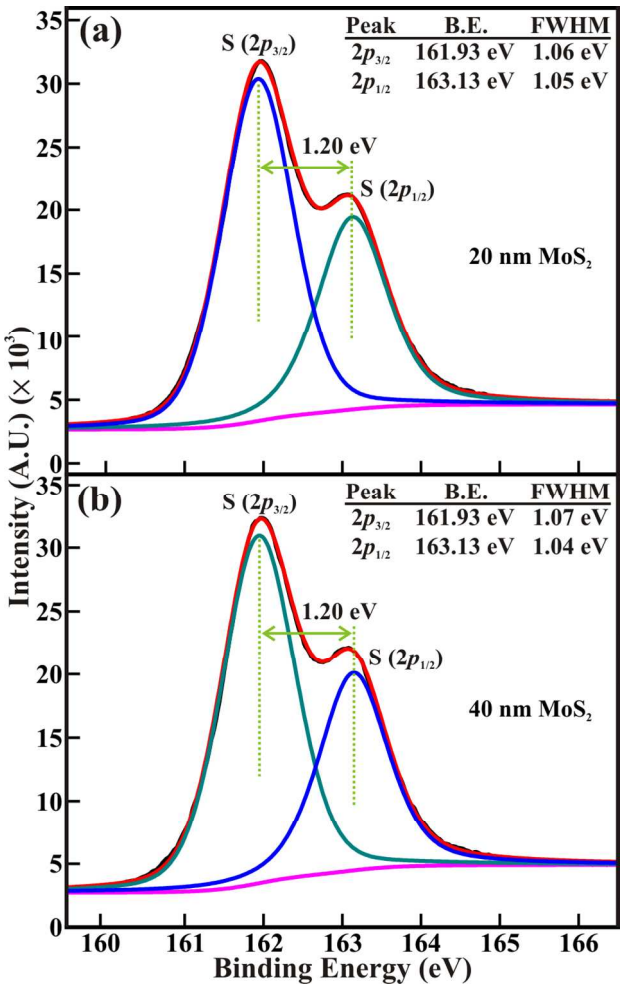

Figure S4. The deconvoluted XPS spectra of S (*2p*) core levels of (a) ~ 20 nm and (b) ~ 40 nm thick MoS_2 loaded β-TiO_2 nanorods. The XPS spectra are deconvoluted *via* Voigt curve function fitting.

(D) Field Emission of pure 2D MoS_2:

FE measurements on 40 nm thick layer of pristine 2D MoS_2 (≡2D MoS_2/Si) were performed in a planar diode configuration. The macroscopic area of the emitting device was ~0.30 cm^2, and values of the anode-cathode separation used were akin to that of pristine β-TiO_2 nanorods i.e. 1000, 1500 and 2000 μm. The variation in the macroscopic electron emission current density (*J*) as a function of applied electric field (*E*) shown in Figure S5(a). The emission

current increased rapidly with the gradual increase in applied voltage. The larger emission current density of ~ 30, 22 and 19 μA/cm^2 was drawn at an applied field of 8.4, 6 and 4.6 V/μm, respectively with an increasing anode-cathode separation from 1000 to 2000 μm. Moreover, the turn-on (E_{on}) field required to extract emission current density of 10 μA/cm^2 was decreased steadily from 7.2 to 4.3 V/μm with an increase in the separation from 500 to 2000 μm. These values of E_{on} are lower than that reported for 3D MoS_2 nanoflowers (4.5-5.5 V/μm) synthesized by reducing MoO_2 thin films in the sulfur atmosphere.[8] Figure S5(b) shows the F-N plot for 2D MoS_2/Si emitter at various separations between anode and cathode. The increase in the separation between cathode and anode commenced for variation in field enhancement factor. The values of β are estimated to be 3905, 4389, 3352, and 1476 for the cathode-anode separations of 1000, 1500 and 2000 μm, respectively. The viability of the field enhancement factor (β_{FE}) of 2D MoS_2/Si emitters was confirmed from orthodoxy text performed using spreadsheet provided by Forbes. [49*] The scaled-barrier-field (f) values obtained for all cathode–anode separations in 2D MoS_2/Si emitters are shown in Table ST1. The emission situation was found orthodox in all cathode–anode separations for both the lower (f_{low}) and highest (f_{high}) scaled-barrier-field values.

Table ST1: The Scaled-barrier-field (f) values evaluated from F-N plots for 40 (± 3 nm) MoS_2/Si emitters obtained using spreadsheet provided in the reference [49]*. Single asterisk on f_{high} values indicates the apparently reasonable values (i.e. $f_{high} < 0.75$).

Separation (μm)	f_{low}	f_{high}	Orthodoxy test result
1000	0.32	0.68	Pass
1500	0.25	0.43	Pass
2000	0.21	0.32	Pass

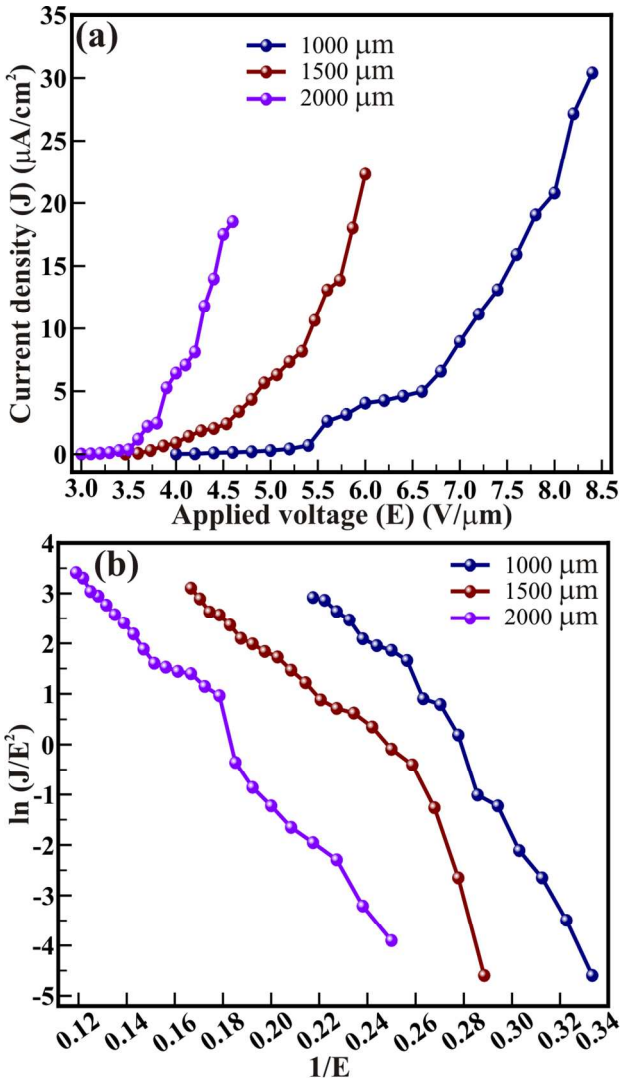

Figure S5. Field emission (a) J-E curves of a large area array of 40 (±3) nm thick layers of pristine 2D MoS_2 (≡2D MoS_2/Si) measured at various vacuum separation (i.e. 1000, 1500, and 2000 μm), and their corresponding (b) F-N plots indicating the emission current.

Table ST2. Comparison of the MoS_2/β-TiO_2/Si emitters with the existing Field emitters utilizing pristine metal oxides and their composites.

Sr. No.	Materials	Turn-on field (E_{on})		Threshold field (E_{thr})		Orthodoxy Test	Ref.
		Observed	Defined	Observed	Defined		
		V/μm	μA/cm^2	V/μm	μA/cm^2		
1.	2D MoS_2@1D β-TiO_2 nanorods	2.5	10	3.6	100	Pass	
2.	MoS_2 protrusions	2.8	10	-	-	Not performed	[48]*
3.	MoS_2 sheets	3.5	10	-	-	Not performed	[19]*
4.	C doped TiO_2 nanotubes	5.0	10	-	-	Not performed	[14]*
5.	Fe doped TiO_2 nanotubes	12	10			Not performed	[13]*
6.	3.88 % N doped TiO_2 nanotubes	10	> 33	11.76	1000	Not performed	[6]*
7.	4.12 % N doped TiO_2 nanotubes	9.21	> 33	14.61	1000	Not performed	[6]*
8.	4.74 % N doped TiO_2 nanotubes	6.54	> 33	20.43	1000	Not performed	[6]*
9.	TiO_2-based TiO_2@MoS_2 composites (flower like spheres)	3.1 - 2.5	01	7.2 - 4.5	100	Not performed	[23]*
10.	MoS_2-based MoS_2@TiO_2 composites (hierarchical spheres)	4 - 2.2	01	6.1 - 3.6	100	Not performed	[23]*
11.	TiO_2 nanorods	14	10	20	100	Not performed	[24]*
12.	MoS_2@TiO_2 nanorods heterostructure	11	10	17	100	Not performed	[24]*
13.	MoS_2 nanoflowers	3.65	10	9.03	1000	Not performed	[20]*
14.	MoS_2@ZnO heterojunctions	3.08	10	6.9	1000	Not performed	[20]*
15.	MoS_2 nanoflowers	4.2	01	6.2	100	Not performed	[21]*
16.	MoS_2@SnO_2 hetero-nanoflowers	3.4	01	5.2	100	Not performed	[21]*

* References are cited in the main text of the manuscript

References

1. Iliev, M. N.; Hadjiev, V. G.; Litvinchuk, A. P., Raman and infrared spectra of brookite (TiO^2): Experiment and theory. *Vib. Spectrosc.,* **2013**, *64*, 148– 152.

2. Pan, H.; Qiu, X. F.; Ivanov, I. N.; Meyer, H. M.; Wang, W.; Zhu, W. G.; Paranthaman, M. P.; Zhang, Z.; Eres, G.; Gu, B. H., Fabrication and characterization of brookite-rich, visible light-active TiO2 films for water splitting. *Appl. Catal. B: Environm.*, **2009**, *93*, 90–95.

3. Hu, Y.; Tsai, H. L.; Huang, C. L., Effect of Brookite Phase on the Anatase-Rutile Transition in Titania Nanoparticles. *J. Eur. Ceram. Soc.*, **2003**, *23*, 691–696.

4. Hu, W. B.; Li, L. P.; Li, G. S.; Tang, C. L.; Sun, L., High-Quality Brookite TiO_2 Flowers: Synthesis, Characterization, and Dielectric Performance. *Cryst. Growth Des.*, **2009**, *9*, 3676–3682.

5. King, L. A.; Zhao, W. J.; Chhowalla, M.; Jason Riley, D.; Eda, G.; Photoelectrochemical properties of chemically exfoliated MoS_2. *J. Mater. Chem. A*, **2013**, *1*, 8935-8941.

6. Lan, F. F.; Lai, Z. P.; Yan, R.; Xu, Y. K.; Cheng, H. J.; Zhang, S.; Chen, J.; Jia, Z. Y.; Wang, Z.; Qi, C. J., Epitaxial Growth of Single-Crystalline Monolayer MoS_2 by Two-Step Method. *ECS Solid State Lett.*, **2015**, *4*, P19-P21.

7. Ambrosi, A.; Sofer, Z.; Pumera, M., Lithium Intercalation Compound Dramatically Influences the Electrochemical Properties of Exfoliated MoS_2. *Small*, **2015**, *11*, 605-612.

8. Li, Y. B.; Bando, Y.; Golberg, D., MoS_2 nanoflowers and their field-emission properties. *Appl. Phys. Lett.*, **2003**, *82*, 1962-1964.